International Journal of Mathematical Research
2025 Vol. 14, No. 1, pp. 1-22.
ISSN(e): 2306-2223
ISSN(p): 2311-7427
DOI: 10.18488/24.v14i1.4665

Stability analysis of a nonlinear tumor–healthy–immune cell model under radiotherapy and chemotherapy

Nicholus Murimi[1]
Jimrise Ochwach[2+]
Daniel Mwangi[3]
Alex Muthengi[4]

[1,3,4]*Department of Basic science, Tharaka University, Marimanti, Kenya.*
[1]*Email: nicholasmurimiwaithega@gmail.com*
[3]*Email: daniel.muriithi@gmail.com*
[4]*Email: alex.mugwiria@gmail.com*
[2]*Department of Computing and Information Technology, Mama Ngina University College, Kiambu, Kenya.*
[2]*Email: ojimrise09@mail.com*


(+ Corresponding author)

Article History
Received: 10 October 2025
Revised: 17 November 2025
Accepted: 15 December 2025
Published: 31 December 2025

Keywords
Basic reproduction number
Cancer treatment modeling
Chemotherapy
Lyapunov method
Nonlinear ODE model
Quiescent tumor cells
Radiotherapy
Sensitivity analysis
Stability analysis
Tumor–immune dynamics.

ABSTRACT

This paper develops an analytical framework for a nonlinear dynamical model describing interactions among healthy cells, tumor cells, quiescent tumor cells, and immune cells under radiotherapy and chemotherapy. The system is formulated as a set of nonlinear ordinary differential equations with therapeutic inputs represented as time-dependent functions. The analysis begins by establishing positivity, boundedness, and an invariant region that confines all solutions to biologically meaningful states. Two equilibrium points are identified: the tumor-free equilibrium and the endemic equilibrium. The basic reproduction number is derived using the Next Generation Matrix approach. The local stability of the equilibrium points is examined using the Jacobian matrix and the Routh–Hurwitz criteria. Global stability is proved with Lyapunov's direct method. Sensitivity analysis is performed using the normalized forward sensitivity index to determine the parameters that most influence. The results show that the tumor growth rate and the transformation rate promote tumor persistence. Radiotherapy efficacy and the immune killing rate suppress tumor growth. When the system converges to the tumor-free equilibrium, it represents effective disease control. The findings demonstrate how mathematical stability and sensitivity analysis support the design of treatment protocols. They also provide a basis for evaluating combined radiotherapy–chemotherapy strategies and how these can shift the tumor–immune balance toward recovery.

Contribution/Originality: This study contributes to existing literature by developing and analyzing a nonlinear tumor–healthy–immune model with radiotherapy and chemotherapy. It provides new stability results, derives a closed-form solution, applies Lyapunov global stability, and documents parameter sensitivity effects on treatment success. The paper offers the first integrated analytical–therapeutic framework for this system.

1. INTRODUCTION

Mathematical modelling helps explain tumor–immune interactions and the effects of therapy. Early work relied on logistic and Gompertz growth laws to describe tumor expansion under limited resources [1, 2]. These models captured basic proliferation patterns but did not incorporate immune activity or treatment responses. Subsequent studies introduced immune surveillance through Lotka–Volterra structures and nonlinear cytotoxic mechanisms [3, 4]. These models showed that immune regulation determines whether tumors persist, regress, or oscillate.

Later research incorporated immune activation, saturation effects, and therapy-induced changes. Models with saturating immune-killing terms explained chronic persistence and relapse in cancer [5, 6]. Other work examined

the role of quiescent tumor cells and their reduced sensitivity to therapy, highlighting the need to represent both proliferating and dormant compartments [7].

Cancer development is influenced by genetic and environmental factors, and the interaction between malignant and healthy cells creates complex nonlinear behavior [8]. Mathematical models provide a structured way to describe these interactions, predict treatment outcomes, and explore optimal control strategies. Early theoretical models such as exponential and logistic growth laws [1, 9], offered foundational insight but did not include immune processes or treatment effects. Later extensions incorporated competition for resources and interactions between healthy and tumor cells [10, 11], though many of these models still omitted key immune mechanisms.

Radiotherapy and chemotherapy remain central treatment strategies. Radiotherapy damages DNA and induces tumor cell death, but can also harm healthy tissue when dosing is not well controlled [12]. Chemotherapy targets rapidly dividing cells but causes toxicity in normal tissues [13]. Models that combine both treatments allow analysis of synergistic effects and support the design of effective therapy schedules.

Stability analysis and threshold measures, such as the basic reproduction number, help determine whether tumors persist or are eliminated. The next-generation matrix method remains a standard tool for deriving these thresholds [14-16]. Models that include healthy tissue, tumor cells, and immune activity show that stability depends on the balance between proliferation, immune killing, and treatment strength [6, 17]. Broader reviews have documented the relevance of such models to oncology [18-20].

The immune system regulates tumor growth through cytotoxic responses that destroy malignant cells [21]. Tumor cells may evade these responses by entering quiescent states, reducing their vulnerability to treatment and immune attack. Models that incorporate these mechanisms help explain tumor escape and relapse.

Recent studies have developed integrated models that couple healthy tissue, tumor growth, quiescent compartments, immunity, and multiple therapies within a single system [6, 22]. These models support long-term analysis of treatment outcomes and control strategies.

This study develops a nonlinear tumor–healthy–immune model with radiotherapy and chemotherapy treated as time-dependent inputs. The analysis establishes positivity, boundedness, and equilibrium stability, and derives the basic reproduction number. Sensitivity analysis identifies the parameters that most influence tumor persistence or clearance. These results clarify how treatment and immunity shape therapeutic outcomes and support the design of optimized cancer treatment strategies.

2. MODEL FORMULATION

This study develops a compartmental model with four interacting populations: healthy cells (H(t)), tumor cells (T(t)), quiescent tumor cells (Q(t)), and immune cells (I(t)). The model captures key biological processes, including cell proliferation, phenotypic transformation, immune response, and the effects of therapy. No additional compartments are introduced for treatment control. Radiotherapy, chemotherapy, and immunotherapy are represented as time-dependent external inputs that modify the dynamics of the biological compartments.

2.1. Model Assumptions

The model is based on the following assumptions.

i). Healthy cells grow logistically with growth rate r_H and carrying capacity K_H.

ii). A fraction of healthy cells transforms into tumor cells at rate α_1.

iii). Tumor cells proliferate logistically with rate r_T and carrying capacity K_T.

iv). Tumor cells can enter a quiescent (dormant) state at rate β, and revert to an active state at rate γ, especially under favorable conditions.

v). Immune cells attack tumor and quiescent cells with saturating (Michaelis-Menten) kinetics.

vi). Tumor cells stimulate immune cell recruitment. Immune cells decay naturally at rate d_I.

vii). Radiotherapy and chemotherapy damage tumor and quiescent cells and also affect healthy cells.

viii). Radiotherapy effectiveness decays with repeated application due to resistance development.

ix). Immunotherapy enhances immune activity without affecting healthy cells.

2.2. Model Description

The population of healthy cells exhibits logistic growth, characterized by a natural proliferation rate r_H and constrained by a carrying capacity K_H, reflecting the finite availability of resources such as nutrients and space. The logistic growth term $r_H H(1-\frac{H}{K_H})$ ensures that the healthy cell population stabilizes as it nears the environment's capacity. However, healthy cells can transform into tumor cells due to genetic mutations or environmental insults, represented by the term $\alpha_1 H$, where α_1 is the transformation rate from healthy to tumor cells. In addition, treatment modalities such as radiotherapy and chemotherapy can directly damage healthy tissue. This is incorporated into the model by including the radiotherapy-induced death term $\rho_H(t)H$, where $\rho_H(t)$ is the time-dependent rate of radiotherapy damage to healthy cells, and the chemotherapy-induced death term $\chi_H(t)H$, with $\chi_H(t)$ representing the time-dependent toxicity of chemotherapy to healthy cells. These considerations lead to the formulation of the healthy cell dynamics as shown in Equation 1. Similar approaches to modeling healthy-tumor interactions under treatment have been discussed by Kim et al. [23] in the context of optimal therapy strategies. Equation 1 presents the healthy-cell dynamics under logistic growth, transformation into tumor cells, and therapy-induced damage.

$$\frac{dH}{dt} = r_H H\left(1-\frac{H}{K_H}\right) - \alpha_1 H - \rho_H(t)H - \chi_H(t)H \tag{1}$$

The tumor cell population increases through two main processes: transformation from healthy cells at a rate α_1, and intrinsic proliferation modeled by logistic growth with proliferation rate r_T and carrying capacity K_T. Tumor cells also receive additional input from the reactivation of quiescent tumor cells at rate γ, which accounts for cells that re-enter the active cycle under favorable conditions such as hypoxia recovery or nutrient availability. Losses in the tumor population occur due to several mechanisms. Natural tumor cell death is modeled by the parameter β. The immune response contributes to tumor reduction through a saturating cytotoxic effect represented by the Michaelis-Menten-like term $\frac{\eta_T IT}{\kappa_T+T}$, where η_T is the immune killing rate and κ_T is the half-saturation constant. Additionally, tumor cells are targeted by radiotherapy and chemotherapy. The time-dependent killing terms $\rho_T(t)$ and $\chi_T(t)$ represent the rates of tumor cell death due to radiotherapy and chemotherapy, respectively. Altogether, these processes are captured in Equation 2, which models the net rate of change of the tumor cell population over time.

$$\frac{dT}{dt} = \alpha_1 H + r_T T\left(1-\frac{T}{K_T}\right) - \beta T + \gamma Q - \frac{\eta_T IT}{\kappa_T+T} - \rho_T(t)T - \chi_T(t)T \tag{2}$$

The quiescent tumor cell compartment Q represents non-proliferating tumor cells that have entered a temporary dormant state due to unfavorable environmental conditions such as hypoxia or lack of nutrients. These cells arise from the active tumor cell population at a rate β, capturing the transition from the proliferating to the quiescent phase. Quiescent cells can return to the active tumor population at a reactivation rate γ, especially when the environment becomes favorable. They are also susceptible to immune surveillance, and this interaction is represented by a saturating immune clearance term $\frac{\eta_Q IQ}{\kappa_Q+Q}$, where η_Q is the killing rate by immune cells and κ_Q is the half-saturation constant. Both radiotherapy and chemotherapy can partially affect quiescent cells, although typically with lower efficacy than on actively dividing cells. These effects are modeled using time-dependent death rates $\rho_Q(t)$ and $\chi_Q(t)$, respectively. These terms reflect the therapeutic impact of treatment on the dormant cell population. The overall dynamics of quiescent cells are summarized in Equation 3, describing the net rate of change of the quiescent tumor cell population over time.

$$\frac{dQ}{dt} = \beta T - \gamma Q - \frac{\eta_Q IQ}{\kappa_Q+Q} - \rho_Q(t)Q - \chi_Q(t)Q \tag{3}$$

The immune cell population I represents cytotoxic immune cells responsible for identifying and eliminating tumor and quiescent cells. Their dynamics are influenced by several biological processes. The term s_I represents the basal source or natural influx of immune cells into the tumor microenvironment, maintaining a minimal level of immune surveillance. The function $\sigma_I(t)$ accounts for externally administered immunotherapy, which boosts the immune population over time through medical intervention. Immune cells can also proliferate in response to tumor presence. This activation and clonal expansion is captured by the term $\frac{\delta T}{\theta+T}I$, a saturating function that models stimulation of immune cells by tumor antigens. Here, δ is the maximum activation rate and θ is the tumor density at which immune activation is half-maximal. Immune cells also undergo natural degradation at a rate d_I, which reflects the finite lifespan of immune effectors and their exhaustion during prolonged engagement. Together, these processes describe the evolution of the immune population in the tumor microenvironment, and Equation 4 outlines the resulting immune-cell dynamics driven by basal influx, immunotherapy, tumor-induced activation, and natural decay.

$$\frac{dI}{dt} = s_I + \sigma_I(t) + \frac{\delta T}{\theta + T}I - d_I I \quad (4)$$

2.3. Model Equations

The proposed model captures the interactions among the four key compartments: healthy cells $H(t)$, tumor cells $T(t)$, quiescent cells $Q(t)$, and immune cells $I(t)$. Healthy cells grow logistically with intrinsic rate r_H and carrying capacity K_H, and are reduced by natural decay $\alpha_1 H$, radiotherapy-induced death $\rho_H(t)H$, and chemotherapy-induced death $\chi_H(t)H$. Tumor cells arise from the transformation of healthy cells at rate $\alpha_1 H$, grow logistically with rate r_T and capacity K_T, and are reduced by transition to quiescence (βT), immune-mediated cytotoxicity ($\frac{\eta_T IT}{\kappa_T+T}$), radiotherapy ($\rho_T(t)T$), and chemotherapy ($\chi_T(t)T$). Quiescent cells are derived from tumor cells at rate βT, and may revert to active tumor phenotype at rate γQ. They are also subject to immune elimination ($\frac{\eta_Q IQ}{\kappa_Q+Q}$), radiotherapy ($\rho_Q(t)Q$), and chemotherapy ($\chi_Q(t)Q$). Immune cells are maintained via basal influx s_I, enhanced by immunotherapy input $\sigma_I(t)$, and proliferate in response to tumor presence via a saturating function $\frac{\delta T}{\theta+T}I$, but decay at rate $d_I I$. Equation 5 summarizes the complete tumor–healthy–immune system as four coupled nonlinear ODEs that model the host–tumor–immune interactions under therapeutic interventions

$$\begin{aligned}
\frac{dH}{dt} &= r_H H\left(1 - \frac{H}{K_H}\right) - \alpha_1 H - \rho_H(t)H - \chi_H(t)H \\
\frac{dT}{dt} &= \alpha_1 H + r_T T\left(1 - \frac{T}{K_T}\right) - \beta T + \gamma Q - \frac{\eta_T IT}{\kappa_T + T} - \rho_T(t)T - \chi_T(t)T \\
\frac{dQ}{dt} &= \beta T - \gamma Q - \frac{\eta_Q IQ}{\kappa_Q + Q} - \rho_Q(t)Q - \chi_Q(t)Q \\
\frac{dI}{dt} &= s_I + \sigma_I(t) + \frac{\delta T}{\theta + T}I - d_I I
\end{aligned} \quad (5)$$

3. RESULTS AND DISCUSSION

3.1. Parameter Estimation

As shown in Table 1, some of the parameter values were estimated, while others were taken from the literature.

Table 1. Parameter values used in the model.

Symbol	Parameter Description	Value	Source
rH	Healthy cell growth rate	0.20 day^{-1}	Kim, et al. [24]
K_H	Healthy tissue carrying capacity	1.0×10^6 cells	Assumed tissue scale
α_1	Transformation rate $H \rightarrow T$	1.0×10^{-7} day^{-1}	De Pillis, et al. [5]
rT	Tumour cell growth rate	0.18 day^{-1}	De Pillis, et al. [5]
K_T	Tumour carrying capacity	1.0×10^6 cells	Standard scaling
β	Transition $T \rightarrow Q$	0.02 day^{-1}	Assumed (quiescence)
γ	Reactivation $Q \rightarrow T$	0.01 day^{-1}	Dormancy assumption
η_T	Immune killing rate (T))	0.50 (dimensionless)	De Pillis, et al. [5]

κ_T	Half-saturation for T kill	1.0×10^5 cells	Literature value
ηQ	Immune killing rate (Q))	0.10 (dimensionless)	Assumed lower efficacy
κQ	Half-saturation for Q kill	1.0×10^5 cells	Literature value
s_I	Basal immune influx	10 cells/day	Typical immune recruitment
σ_I	Immunotherapy influx	5 cells/day	Assumed moderate boost
δ	Max immune recruitment rate	0.10 day^{-1}	Kim, et al. [24]
θ	Tumour load for half-maximal activation of the immune system	5.0×10^4 cells	Kim, et al. [24]
d_I	Immune decay rate	0.10 day^{-1}	Typical immune lifespan
ρH	Radiotherapy death rate (healthy)	0.02 day^{-1}	Assumed collateral damage
ρ_T	Radiotherapy death rate (tumour))	0.10 day^{-1}	Literature typical
ρQ	Radiotherapy death rate (quiescent)	0.02 day^{-1}	Assumed lower sensitivity
χH	Chemotherapy death rate (healthy)	0.01 day^{-1}	Assumed toxicity to normal cells
χ_T	Chemotherapy death rate (tumour)	0.05 day^{-1}	Literature typical
χ_Q	Chemotherapy death rate (quiescent)	0.01 day^{-1}	Assumed lower sensitivity

3.2. Boundedness and Positivity of Solutions

Maintaining the biological viability of differential equation solutions is crucial when modeling biological systems. Proving the positivity and boundedness of solutions is usually how this is accomplished. Population variables such as immune cells (I), tumor cells (T), healthy cells (H), and quiescent tumor cells (Q) are protected from achieving negative values through positivity. Boundedness guarantees that these variables do not grow unbounded over time, respecting biological and physical constraints such as carrying capacities and resource limitations.

Considering the system of equations defined in (5), subject to non-negative initial conditions.

$$H(0) \geq 0, \quad T(0) \geq 0, \quad Q(0) \geq 0, \quad I(0) \geq 0.$$

3.3. Positivity of Solutions

In order for the model to be biologically meaningful, it is necessary to show that the solutions with nonnegative initial conditions remain nonnegative for all time $t \geq 0$. This property guarantees that the state variables, which represent population densities of cells, do not take negative values during the system's evolution.

Theorem 3.1. Let the initial conditions of system (5) satisfy.

$$H(0) \geq 0, \quad T(0) \geq 0, \quad Q(0) \geq 0, \quad I(0) \geq 0.$$

Then the solutions $(H(t), T(t), Q(t), I(t))$ of system (5) remain nonnegative for all $t \geq 0$.

Proof. Consider the first equation of system (5). At $H = 0$, we obtain Equation 6.

$$\left.\frac{dH}{dt}\right|_{H=0} = r_H H\left(1 - \frac{H}{K_H}\right) - \alpha_1 H - \rho_H(t)H - \chi_H(t)H\Big|_{H=0} = 0 \tag{6}$$

Thus, $H(t)$ cannot cross the plane $H = 0$ from the nonnegative region to the negative region.

Similarly, at $T = 0$, the second equation yields Equation 7.

$$\left.\frac{dT}{dt}\right|_{T=0} = \alpha_1 H + r_T T\left(1 - \frac{T}{K_T}\right) - \rho_T(t)T - \chi_T(t)T\Big|_{T=0} \geq 0 \tag{7}$$

Since $H \geq 0$. Therefore, $T(t)$ cannot become negative.

Proceeding analogously for Q and I, we observe that the vector field on the boundary of the nonnegative orthant points inward or is tangent to the boundary. Hence, the nonnegative orthant $\mathbb{R}^4_+$ is positively invariant under the flow of system (5).

The above theorem ensures that the model remains biologically well-posed, since the solutions starting with nonnegative initial conditions are guaranteed to remain in the feasible region $\mathbb{R}^4_+$ for all $t \geq 0$. This provides a sound basis for the subsequent stability and bifurcation analyses.

3.4. Boundedness of Solutions

In addition to positivity, it is essential to demonstrate that the solutions of system (5) are bounded. This guarantees that the populations of healthy, tumour, quiescent, and immune cells remain within biologically realistic limits for all future times, thereby ensuring the mathematical and biological well-posedness of the model.

Theorem 3.2. All solutions of system (5) with nonnegative initial conditions are uniformly bounded in $\mathbb{R}^4_+$.

Proof. Consider the total population, Equation 8:

$$W(t) = H(t) + T(t) + Q(t) + I(t). \tag{8}$$

Differentiating with respect to time and using system (5), we obtain Equation 9:

$$\frac{dW}{dt} = \frac{dH}{dt} + \frac{dT}{dt} + \frac{dQ}{dt} + \frac{dI}{dt}. \tag{9}$$

From the healthy cell equation, we have Equation 10:

$$\frac{dH}{dt} \leq r_H H \left(1 - \frac{H}{K_H}\right). \tag{10}$$

Thus, $H(t)$ is bounded above by the healthy cell carrying capacity K_H.

For the tumour population, combining the proliferating and quiescent compartments yields Equation 11.

$$\frac{d}{dt}(T+Q) \leq r_T T \left(1 - \frac{T}{K_T}\right), \tag{11}$$

Implying $T(t) + Q(t)$ is bounded above by the tumour carrying capacity K_T.

For the immune cell population, we have Equation 12.

$$\frac{dI}{dt} \leq s_I + \sigma_I + \delta I - d_I I. \tag{12}$$

By comparison with the linear equation $y' = (\delta - d_I)y + (s_I + \sigma_I)$, it follows that.

$$I(t) \leq \frac{s_I + \sigma_I}{d_I - \delta} \tag{13}$$

Whenever $d_I > \delta$.

Hence, each compartment is bounded above by a biologically realistic constant. Consequently, yielding to Equations 14 - 16.

$$0 \leq H(t) \leq K_H \tag{14}$$

$$0 \leq T(t) + Q(t) \leq K_T \tag{15}$$

$$0 \leq I(t) \leq \frac{s_I + \sigma_I}{d_I - \delta} \tag{16}$$

Therefore, $W(t)$ is uniformly bounded, which establishes the boundedness of all solutions of system (5).

The above theorem ensures that the trajectories of system (5) remain confined within a compact subset of $\mathbb{R}^4_+$. This boundedness result is crucial because it rules out the possibility of unbounded growth in any of the compartments, thereby confirming the biological consistency of the model and preparing the ground for the analysis of invariant regions.

3.5. Invariant Region

For biological realism, it is important to show that the solutions of system (5) not only remain nonnegative but are also uniformly bounded. This ensures that the cell populations do not grow without limit and that the system dynamics are confined to a biologically feasible region.

Theorem 3.3. The region

$$\Omega = \left\{(H,T,Q,I) \in \mathbb{R}^4_+ \ : \ 0 \leq H \leq K_H, \right. \tag{17}$$

$$0 \le T + Q \le K_T, \quad 0 \le I \le \frac{s_I + \sigma_I}{d_I} + M \Big\} \tag{18}$$

Where $M > 0$ is a constant depending on the proliferation parameters, it is positively invariant with respect to system (5).

Proof. From the first equation of system (5), the healthy cell population satisfies Equation 19.

$$\frac{dH}{dt} \le r_H H \left(1 - \frac{H}{K_H}\right) \tag{19}$$

By comparison, $H(t)$ is bounded above by the logistic equation with carrying capacity K_H, hence $H(t) \le K_H$ for all $t \ge 0$.

For the tumour compartment, adding the second and third equations gives Equation 20.

$$\frac{d}{dt}(T + Q) \le r_T T \left(1 - \frac{T}{K_T}\right) - \rho_T T - \chi_T T - \rho_Q Q - \chi_Q Q, \tag{20}$$

Which shows that $T + Q$ is bounded above by the tumour carrying capacity K_T.

For the immune cell population, Equation 21:

$$\frac{dI}{dt} \le s_I + \sigma_I + \delta I - d_I I, \tag{21}$$

Which implies $I(t)$ is bounded above by a constant of the form $\frac{s_I + \sigma_I}{d_I} + M$.

Thus, trajectories starting in Ω remain in Ω for all $t \ge 0$, proving that Ω is positively invariant.

The theorem guarantees that all solutions of system (5) eventually enter and remain in the compact set $\Omega \subset \mathbb{R}^4_+$. This ensures that the model is mathematically well-posed and biologically meaningful, and provides the feasible region within which stability and bifurcation analyses can be carried out.

3.6. Equilibrium Analysis

Two biologically relevant types of equilibria are examined in this work: the tumor-free equilibrium (TFE) and the tumor-present equilibrium (TPE), which indicate a disease-free state where tumor cells are completely absent from the system and a persistent coexistence of tumor, healthy, and immune cells, respectively. These equilibria provide important information about the system's long-term behavior and the efficacy of therapeutic interventions. To determine the equilibrium points of the system, the right-hand sides of system (5) are set to zero, as shown in Equation 22.

$$\frac{dH}{dt} = \frac{dT}{dt} = \frac{dQ}{dt} = \frac{dI}{dt} = 0 \tag{22}$$

3.7. Tumour-Free Equilibrium (TFE)

To investigate the existence of a tumor-free state, the tumor compartments of the model system are set to zero, that is, T = Q = 0. The reduced system for healthy cells (H) and immune cells (I) is then simplified as shown in equation (23).

$$H = r_H H \left(1 - \frac{H}{K_H}\right) - (\rho_H + \chi_H) H, \tag{23}$$

$$I = s_I + \sigma_I - d_I I. \tag{24}$$

Equation () describes logistic-type growth for the healthy population, modified by the natural loss rate ρ_H and therapy-induced depletion χ_H. Equation 23 represents the balance between immune cell supply ($s_I + \sigma_I$) and natural decay (d_I). A necessary condition for a valid tumor-free state is the absence of spontaneous inflow into the tumor class from healthy cells. This requires that.

$$\alpha_1 = 0 \tag{25}$$

Otherwise, tumor cells would continuously reappear from the healthy pool. Under condition (25), the tumor-free equilibrium is as illustrated in Equation 27.

$$E_0 = (H^*, 0, 0, I^*), \quad (26)$$

With steady states

$$H^* = K_H\left(1 - \frac{\alpha_1 + \rho_H^* + \chi_H^*}{r_H}\right) \quad (27)$$

$$I^* = \frac{s_I + \sigma_I^*}{d_I}. \quad (28)$$

For biological feasibility, $H^* > 0$ must hold, which is equivalent to the condition in Equation 29.

$$r_H > \rho_H + \chi_H. \quad (29)$$

This ensures that the intrinsic growth rate of healthy tissue exceeds the combined natural and therapeutic losses, guaranteeing the persistence of H in the absence of tumor cells.

3.8. Endemic Equilibrium (EE)

At the endemic equilibrium $E_1^* = (H^{**}, T^{**}, Q^{**}, I^{**})$, the tumor persists in the system and all compartments attain non-zero steady states with $T^{**}, Q^{**}, I^{**} > 0$. The steady state is obtained by setting the right-hand sides of system (5) to zero, while evaluating the time-dependent therapeutic controls at their long-term values $\rho_H, \chi_H, \rho_T, \chi_T, \rho_Q, \chi_Q, \sigma_I$. The resulting algebraic system is as shown in Equations 30 - 33.

$$0 = r_H H\left(1 - \frac{H^{**}}{K_H}\right) - \alpha_1 H - \rho_H H - \chi_H H, \quad (30)$$

$$0 = \alpha_1 H + r_T T\left(1 - \frac{T^{**}}{K_T}\right) - \beta T + o\gamma Q - \frac{\eta_T I T}{\kappa_T + T^{**}} - \rho_T T - \chi_T T, \quad (31)$$

$$0 = \beta T - \gamma Q - \frac{\eta_Q I Q}{\kappa_Q + Q^{**}} - \rho_Q Q - \chi_Q Q, \quad (32)$$

$$0 = s_I + \sigma_I + \frac{\delta T}{\theta + T^{**}} I^{**} - d_I I. \quad (33)$$

Solving these equations sequentially to express each equilibrium component in terms of the tumor population T^{**}, thereby reducing the system to a single closure equation, which mirrors the analytical approach commonly used in tumor-immune modeling.

From Equation 30, assuming $H^{**} > 0$, the equation yield Equation 34.

$$H^{**} = K_H \frac{r_H - (\alpha_1 + \rho_H + \chi_H)}{r_H}. \quad (34)$$

A biologically meaningful H^{**} requires.

$$r_H > \alpha_1 + \rho_H + \chi_H. \quad (35)$$

This Equation 35 inequality represents a natural threshold: the intrinsic regeneration of healthy tissue must outweigh the combined losses due to tumor invasion (α_1) and therapy-induced cytotoxicity (ρ_H, χ_H). If violated, the healthy cell population collapses, signifying tissue damage or treatment toxicity.

From Equation 33, we isolate I^{**} as shown in Equation 36.

$$I^{**} = \frac{s_I + \sigma_I}{d_I - \frac{\delta T}{\theta + T^{**}}} \quad (36)$$

The condition for positivity is $d_I > \delta T/(\theta + T^{**})$. Biologically, this balance shows that immune cells are sustained through baseline recruitment (s_I) and therapeutic stimulation (σ_I). The tumor load T^{**} contributes additional activation, but excessive tumor burden can overwhelm immune persistence if $\delta T/(\theta + T^{**})$ approaches d_I.

Equation 32 reduces to a quadratic form in Q^{**}. Setting $R_2 = \gamma + \rho_2 + \chi_2$ and solving yields Equation 37;

$$Q^{**}(T^{**}) = \frac{\beta T^{-} R_Q \kappa_Q - \eta_Q I(T^{**}) + \sqrt{\left(\beta T - R_Q \kappa_Q - \eta_Q I(T^{**})\right)^2 + 4 R_Q \beta T \kappa_Q}}{2 R_Q} \tag{37}$$

where $I^{**}(T^{**})$ is substituted from (36). The positive root is taken to ensure biological relevance. This expression shows that the quiescent population is maintained by transition from the active tumor compartment (βT), balanced against immune clearance ($\eta_2 I$) and reactivation into proliferating tumor cells (γ). The persistence of Q^{**} reflects tumor dormancy, a mechanism often linked to recurrence after apparent remission.

Considering Active tumor cells T^{**}. and finally, substituting H^{**}, $I^{**}(T^{**})$, and $Q^{**}(T^{**})$ into (31), we define the scalar closure equation.

$$F(T^{**}) = \alpha_1 H + r_T T\left(1 - \frac{T^{**}}{K_T}\right) - (\beta + \rho_T + \chi_T) T^{**} + \gamma Q(T^{**}) - \frac{\eta_T I(T^{**}) T^{**}}{\kappa_T + T^{**}} \tag{38}$$

The endemic equilibrium tumor burden $T^{**} > 0$ is determined by solving $F(T^{**}) = 0$. Once T^{**} is determined, the corresponding H^{**}, Q^{**}, I^{**} are uniquely obtained from Equations 34 and 37, yielding.

$$E_1^* = \left(H^{**}, T^{**}, Q^{**}(T^{**}), I^{**}(T^{**})\right) \tag{39}$$

Thus, the endemic equilibrium not only provides a mathematical condition for tumor persistence but also yields biologically interpretable thresholds for treatment efficacy and disease progression.

3.9. Basic Reproduction Number R_0

To assess the potential for tumor invasion, the next-generation matrix (NGM) method is applied [14, 25]. The infected subsystem is identified as $x(t) = (T,Q)^{\top}$ where T and Q denote proliferating and quiescent tumor cells, respectively. The subsystem dynamics can be written as. Equation 40 expresses the infected subsystem in next-generation matrix form, separating new tumor production from all other transitions.

$$\frac{d\mathbf{x}}{dt} = \mathcal{F}(\mathbf{x}) - \mathcal{V}(\mathbf{x}) \tag{40}$$

Where F(**x**) contains new tumor proliferation terms and V(**x**), accounts for all other transfers including progression, regression, death, and immune-mediated killing. The new infection vector is. Equation 41 presents the vector of new tumor cell production rates.

$$\mathcal{F}(\mathbf{x}) = \begin{pmatrix} r_T T \\ 0 \end{pmatrix} \tag{41}$$

While the transition vector is.

$$V(x) = \begin{pmatrix} (\beta + (\rho_T + \chi_T)^T - \gamma_Q + \frac{\eta_T I T}{\kappa_T + T} \\ -\beta T + (\gamma + \rho_Q + \chi_Q)^Q + \frac{\eta_Q I Q}{\kappa_Q + Q} \end{pmatrix}. \tag{42}$$

Equation 42 defines the transition vector containing loss, movement, and immune-mediated clearance terms. At E_0, the nonlinear immune terms are linearized, yielding the effective per capita killing rates.

The Jacobian matrices of F and V at E_0 are given in Equations 43 and 44.

$$F = \begin{pmatrix} r_T & 0 \\ 0 & 0 \end{pmatrix}, \tag{43}$$

$$V = \begin{pmatrix} a & -\gamma \\ -\beta & d \end{pmatrix}. \tag{44}$$

Where,

$$a = \beta + \rho_T + \chi_T + \frac{\eta_T I^*}{\kappa_T}, \tag{45}$$

$$d = \gamma + \rho_Q + \chi_Q + \frac{\eta_Q I^*}{\kappa_Q} \tag{46}$$

The next-generation matrix is given by Equation 47.

$$K = FV^{-1} \quad (47)$$

The invertibility of V requires the determinant condition, which is given by Equation 48.

$$ad - \beta\gamma > 0 \quad (48)$$

Which also guarantees that V is an M-matrix and ensures the positivity of the inverse.

The inverse of V yields Equation 49.

$$(V')^{-1} = \frac{1}{ad - \beta\gamma}\begin{pmatrix} d & \gamma \\ \beta & a \end{pmatrix}. \quad (49)$$

This yields the next-generation matrix given by Equation 50

$$K = \frac{r_T}{ad - \beta\gamma}\begin{pmatrix} d & \gamma \\ 0 & 0 \end{pmatrix} \quad (50)$$

Whose eigenvalues are given by Equations 51 and 52.

$$\lambda_1 = \frac{r_T d}{ad - \beta\gamma} \quad (51)$$

$$\lambda_1 = \frac{r_T d}{ad - \beta\gamma} \quad (52)$$

Hence, the basic reproduction number is given by Equation 53.

$$R_0 = \frac{r_T d}{ad - \beta\gamma} \quad (53)$$

Substituting Equations 50, 53 yields the complete basic reproduction number given in Equation 54.

$$R_0 = \frac{r_T\left(\gamma + \rho_Q + \chi_Q + \frac{\eta_Q(s_I + \sigma_I)}{d_I\kappa_Q}\right)}{\left(\beta + \rho_T + \chi_T + \frac{\eta_T(s_I + \sigma_I)}{d_I\kappa_T}\right)\left(\gamma + \rho_Q + \chi_Q + \frac{\eta_Q(s_I + \sigma_I)}{d_I\kappa_Q}\right) - \beta\gamma} \quad (54)$$

3.10. Local Stability Analysis of TFE

For analytical clarity, we first set $\alpha_1 = 0$, removing continual exogenous seeding from healthy to tumour cells. With $T = Q = 0$, the system admits the tumour-free equilibrium in Equation 55.

$$E_0 = (H^*, 0, 0, I^*), \qquad H^* = K_H\left(1 - \frac{\rho_H + \chi_H}{r_H}\right), \qquad I^* = \frac{s_I + \sigma_I}{d_I} \quad (55)$$

Which is biologically feasible provided $r_H > \rho_H + \chi_H$.

The computation of the Jacobian matrix of system (5) at E_0 results in Equation 56

with

$$J(E_0) = \begin{pmatrix} a_{11} & 0 & 0 & 0 \\ 0 & a_{22} & \gamma & 0 \\ 0 & \beta & a_{33} & 0 \\ 0 & a_{42} & 0 & -d_I \end{pmatrix} \quad (56)$$

$$\begin{aligned} a_{11} &= -\left(r_H - (\rho_H + \chi_H)\right), \\ a_{22} &= r_T - \beta - \rho_T - \chi_T - \tfrac{\eta_T I^*}{\kappa_T}, \\ a_{33} &= -\gamma - \rho_Q - \chi_Q - \tfrac{\eta_Q I^*}{\kappa_Q}, \\ a_{42} &= \tfrac{\delta I^*}{\theta}. \end{aligned} \quad (57)$$

Two eigenvalues are immediate: $a_{11} < 0$ (under feasibility) and $-d_I < 0$. Thus, stability reduces to the 2×2 tumour–quiescent Equation 58.

$$M = \begin{pmatrix} a_{22} & \gamma \\ \beta & a_{33} \end{pmatrix} \quad (58)$$

Defining;

$$a := \beta + \rho_T + \chi_T + \frac{\eta_T I^*}{\kappa_T}, \qquad d := \gamma + \rho_Q + \chi_Q + \frac{\eta_Q I^*}{\kappa_Q} \quad (59)$$

so that $a_{22} = r_T - a$ and $a_{33} = -d$. The characteristic polynomial of M is Equation 60.

$$\lambda^2 - (a_{22} + a_{33})\lambda + (a_{22}a_{33} - \beta\gamma) = 0 \quad (60)$$

By the Routh–Hurwitz criterion, both roots have negative real parts if and only if Equation 61 holds.

$$a_{22} + a_{33} < 0 \quad \text{and} \quad a_{22}a_{33} - \beta\gamma > 0. \quad (61)$$

The determinant condition simplifies to Equation 62.

$$d(r_T - a) + \beta\gamma < 0 \quad (62)$$

which is equivalent to Equation 63.

$$\frac{r_T d}{ad - \beta\gamma} < 1 \quad (63)$$

We therefore define the effective tumour reproduction number as shown in Equation 64.

$$R_0 := \frac{r_T d}{ad - \beta\gamma}, \ (ad - \beta\gamma > 0). \quad (64)$$

Theorem 3.4. Suppose $\alpha_1 = 0$ and $r_H > \rho_H + \chi_H$. Let R_0 be as in (64). Then.

1. If $R_0 < 1$, all eigenvalues of $J(E_0)$ are negative, and the tumour-free equilibrium E_0 is locally asymptotically stable.
2. If $R_0 > 1$, $J(E_0)$ has a positive eigenvalue and E_0 is unstable.

Proof. Under feasibility, $a_{11} < 0$ and $-d_I < 0$. The remaining eigenvalues are roots of the quadratic Equation 64 above. Routh–Hurwitz reduces to conditions already shown equivalent to $R_0 < 1$. Hence, $R_0 < 1$ ensures stability of E_0; if $R_0 > 1$, one eigenvalue is positive and E_0 is unstable.

From the equations above and the numerical substitution of the parameter values in Table 4.1, and $\alpha_1 = 0$, it is determined that.

$$I^* = \frac{10 + 5}{0.10} = 150, \quad a \approx 0.17075, \quad d \approx 0.04015, \quad ad - \beta\gamma \approx 0.0066556 > 0 \quad (65)$$

Thus

$$R_0 \approx \frac{0.18 \times 0.04015}{0.0066556} \approx 1.0859 > 1 \quad (66)$$

Indicating that under baseline parameters, the TFE is unstable, and tumor invasion occurs.

The threshold R_0 balances tumor transitions (β,γ) and tumor proliferation (r_T) against immune clearance and therapy (via a,d).

Any minor introduction of tumor cells is eliminated and E_0 is stable if $R_0 < 1$. Tumor cells persist if $R_0 > 1$, which destabilizes E_0. Therefore, increasing immunological stimulation (s,σ_I) and treatment (χ_T,χ_2) reduces R_0 and encourages tumor control.

3.11. Global Stability of the TFE

To complement the local analysis, we now establish conditions for global stability of the tumour-free equilibrium. Consider the Lyapunov candidate function in Equation 67.

$$L(T, Q) = T + Q, \quad (67)$$

Which is positive definite in the tumour subspace (T, $Q \geq 0$) and vanishes only at $T = Q = 0$. Differentiating along the trajectories of the full system yields Equation 68.

$$\frac{d\mathcal{L}}{dt} = \frac{dT}{dt} + \frac{dQ}{dt} \quad (68)$$

Using the tumour equations, this can be expressed in the form given in Equation 69.

$$\frac{d\mathcal{L}}{dt} \leq (R_0 - 1)\,\psi(T, Q) \quad (69)$$

where $\psi(T, Q)$ is a non-negative function representing the effective tumour growth.

Hence, if $R_0 < 1$, we have $\frac{d\mathcal{L}}{dt} < 0$ for all T, $Q > 0$, implying that L(T,Q) decreases monotonically to zero. By LaSalle's

Invariance Principle, all trajectories converge asymptotically to

$$E_0 = (H^*,0,0,I^*). \quad (70)$$

Theorem. The tumour-free equilibrium E_0 exists whenever conditions (25)– (29) hold. Moreover, if $R_0 < 1$, then E_0 is globally asymptotically stable in the feasible region Ω.

The result demonstrates that when the effective reproductive capacity of tumour cells falls below unity, not only is tumour invasion locally prevented, but the entire system evolves globally to a tumour-free state regardless of the initial tumour burden. This highlights the effectiveness of therapeutic and immune mechanisms in ensuring complete tumour eradication.

3.12. Local Stability Analysis of the Endemic Equilibrium

By assessing the local stability of the endemic equilibrium point $E^* = (H^*,T^*,Q^*,I^*)$ of system (5), where all state variables are positive. Let:

$$\mathbf{X}(t) = (H,T,Q,I)^\top \quad (71)$$

The Jacobian matrix $J(E^*)$ of the system evaluated at the endemic equilibrium is given in Equation 72.

$$J(E^*) = \begin{pmatrix} J_{11} & 0 & 0 & 0 \\ J_{21} & J_{22} & J_{23} & J_{24} \\ 0 & J_{32} & J_{33} & J_{34} \\ 0 & J_{42} & 0 & J_{44} \end{pmatrix} \quad (72)$$

The partial derivatives of Equation 72 yields Equation 73.

$$\begin{aligned}
J_{11} &= \frac{\partial f_H}{\partial H} are = r_H\left(1 - \frac{2H^*}{K_H}\right) - \alpha_1 - \rho_H - \chi_H \\
J_{21} &= \frac{\partial f_T}{\partial H} = \alpha_1 \\
J_{22} &= \frac{\partial f_T}{\partial T} = r_T\left(1 - \frac{2T^*}{K_T}\right) - \beta - \rho_T\chi_T - \frac{\eta_T I^* \kappa_T}{(\kappa_T + T^*)^2} \\
J_{23} &= \frac{\partial f_T}{\partial Q} = \gamma \\
J_{24} &= \frac{\partial f_T}{\partial I} = -\frac{\eta_T T^*}{\kappa_T + T^*} \\
J_{32} &= \frac{\partial f_Q}{\partial T} = \beta \\
J_{33} &= \frac{\partial f_Q}{\partial Q} = -\gamma - \rho_Q - \chi_Q - \frac{\eta_Q I^* \kappa_Q}{(\kappa_Q + Q^*)^2} \\
J_{34} &= \frac{\partial f_Q}{\partial I} = -\frac{\eta_Q Q^*}{\kappa_Q + Q^*} \\
J_{42} &= \frac{\partial f_I}{\partial T} = \frac{\delta\theta I^*}{(\theta + T^*)^2} \\
J_{44} &= \frac{\partial f_I}{\partial I} = \frac{\delta T^*}{\theta + T^*} - d_I
\end{aligned} \quad (73)$$

Since $J_{11} < 0$ whenever $r_H > \alpha_1 + \rho_H + \chi_H$, the healthy compartment is locally stable and decouples near equilibrium. Thus, stability of E_1^* is determined by the tumour–quiescent–immune subsystem where the focus is on the 3×3 matrix: Tumor–quiescent–immune subsystem.

$$\mathbf{Y} = (T,Q,I) \quad (74)$$

The subsystem matrix A is shown in Equation 75.

$$A = \begin{pmatrix} J_{22} & J_{23} & J_{24} \\ J_{32} & J_{33} & J_{34} \\ J_{42} & 0 & J_{44} \end{pmatrix} \quad (75)$$

The characteristic polynomial of A is given in Equation 76.

$$\lambda^3 + a_1\lambda^2 + a_2\lambda + a_3 = 0 \quad (76)$$

Lemma 3.1. The endemic equilibrium E_1^* is locally asymptotically stable if

$$a_1 > 0, \quad a_2 > 0, \quad a_3 > 0, a_1a_2 > a_3. \quad (77)$$

Theorem 3.5. If $R_0 > 1$, so that E_1^* exists, and the Routh–Hurwitz conditions in the lemma (3.1) hold, then E_1^* is locally asymptotically stable. Otherwise, it is unstable.

The condition $a_1 > 0$ ensures that overall losses dominate tumour proliferation, $a_2 > 0$ guarantees stabilising pairwise feedbacks (tumour–immune and tumour–quiescent), and $a_3 > 0$ prevents runaway amplification. The inequality $a_1a_2 > a_3$ rules out oscillatory instabilities. The stability of the endemic state therefore requires a delicate balance between tumour proliferation, immune clearance, quiescence dynamics, and therapeutic pressure.

3.13. Global Stability of the Endemic Equilibrium

We now turn to the global dynamics of the endemic equilibrium shown in Equation 78.

$$E_1^* = (H^{**}, T^{**}, Q^{**}, I^{**}), \quad (78)$$

of system (5). Recall that E_1^* exists whenever $R_0 > 1$ and all state variables are strictly positive and by establishing global stability of E_1^* using a Lyapunov approach, we consider the Volterra-type Lyapunov function shown in Equation 79.

$$V(H,T,Q,I) = \sum_{j\in\{H,T,Q,I\}} \left(\frac{j}{j^{**}} - \ln\frac{j}{j^{**}} - 1\right). \quad (79)$$

where j^* denotes the corresponding coordinate of E^*. Each scalar summand is nonnegative and C^1 on $(0,\infty)$ and vanishes only at $j = j^*$. Thus $V \geq 0$ on D and $V = 0$ if and only if $(H,T,Q,I) = E^*$.

Differentiating along solutions of system (5) gives Equation 80.

$$\frac{dV}{dt} = \sum_{j\in\{H,T,Q,I\}} \left(1 - \frac{j^{**}}{j}\right)\frac{1}{j^{**}} \cdot \frac{dj}{dt}. \quad (80)$$

Substituting system equations and using equilibrium conditions ($\dot{H} = \dot{T} = \dot{Q} = \dot{I} = 0$ at E_1^*) shows that

$$\frac{dV}{dt} \leq 0, \qquad \frac{dV}{dt} = 0 \iff (H,T,Q,I) = E_1^*. \quad (81)$$

Since the system is bounded and positively invariant, LaSalle's invariance principle implies.

Theorem 3.6. The endemic equilibrium $E_1^* = (H^{**}, T^{**}, Q^{**}, I^{**})$ of system (5) is globally asymptotically stable in the interior of $\mathbb{R}^4_+$, provided all parameters are positive and constant.

Both the local and global stability of the endemic equilibrium have been examined in this section. E_1^* is locally asymptotically stable whenever $R_0 > 1$, according to the local stability analysis, and the Lyapunov-based global analysis also showed that this stability holds true for the whole feasible region. From a biological perspective, this implies that if tumor cells become established in the host, the system will unavoidably move toward a state of continuous cohabitation between the tumor and host cells. To eradicate tumor cells, the basic reproduction number R_0 must be lowered below unity.

This is the only effective control method.

4. NUMERICAL SIMULATIONS

The nonlinear system of ordinary differential equations defined in Equation 5 was simulated numerically to analyze the dynamics of tumor–host interactions under different therapeutic interventions. Since closed-form solutions are not available, numerical simulations provide insight into the qualitative behavior and long-term outcomes of the system. Parameter values were obtained from published studies, while a few were estimated within biologically plausible ranges. Computations were carried out using Python, and the results are presented graphically. This section presents the baseline dynamics, the effects of radiotherapy and chemotherapy, the role of treatment timing, and the impact of combined therapeutic strategies.

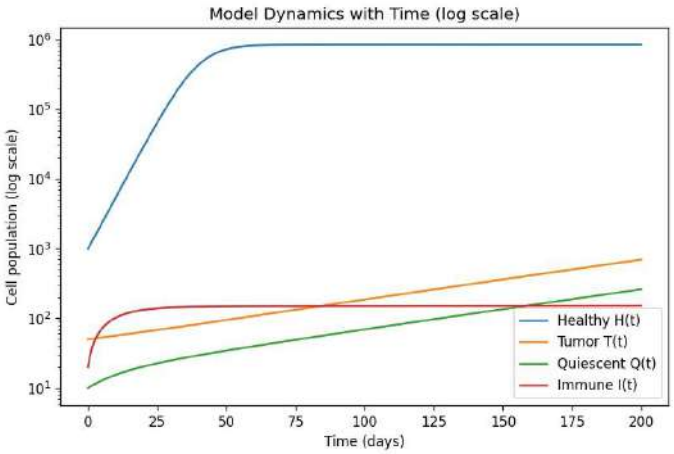

Figure 1. Model dynamics on a logarithmic scale showing the relative sizes of H(t), T(t), Q(t), and I(t) populations.

4.1. Model Dynamics

Figure 1 uses a logarithmic scale to highlight differences in order of magnitude. While $H(t)$ stabilizes near 10^6, tumor cells $T(t)$ and quiescent cells $Q(t)$ remain significantly smaller but continue to increase steadily. Immune cells $I(t)$ show an initial burst followed by a plateau. These dynamics confirm that tumors can persist at low levels even when dominated by healthy tissue.

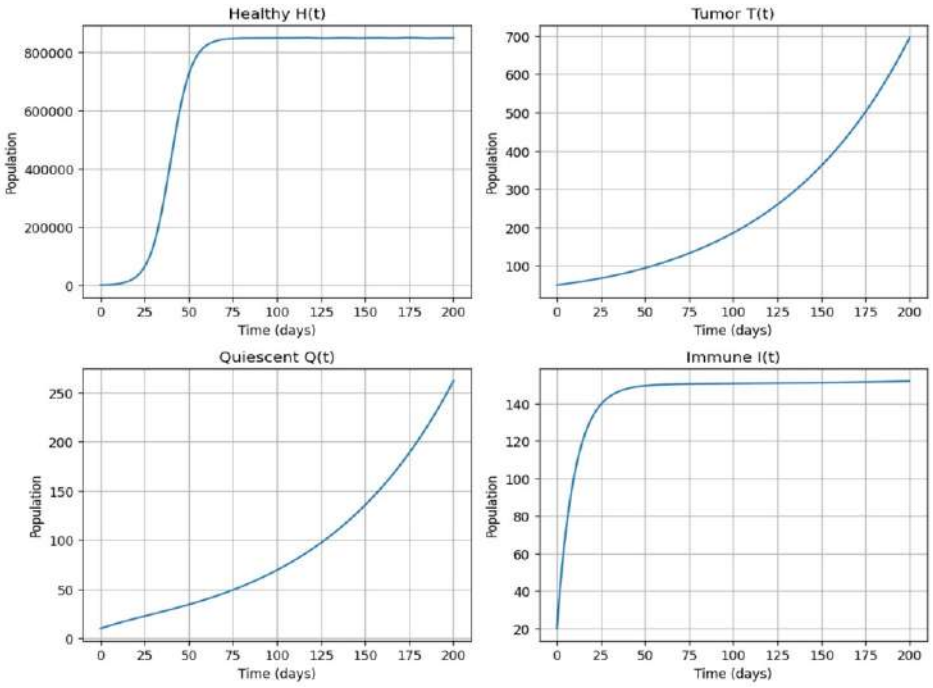

Figure 2. Temporal dynamics of all cell populations under baseline conditions.

As seen in Figure 2, the four populations exhibit distinct temporal patterns consistent with earlier plots: healthy cells dominate, tumor and quiescent cells persist at low levels, and immune cells plateau after an initial response.

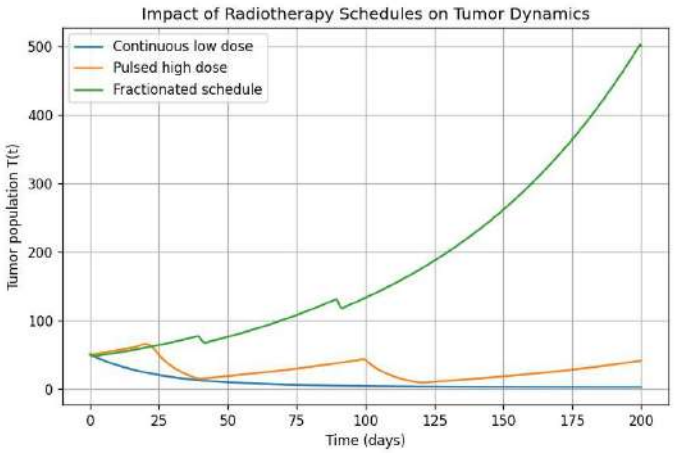

Figure 3. Impact of different radiotherapy schedules on tumor cells T(t): continuous low dose, pulsed high dose, and fractionated delivery.

4.2. Radiotherapy Effects

Figure 3 compares radiotherapy schedules. Continuous low-dose therapy drives tumor levels near zero. Pulsed high-dose therapy produces sharp declines followed by regrowth between cycles, creating oscillatory tumor dynamics. Fractionated therapy moderates growth but fails to achieve eradication. These outcomes highlight that continuous delivery is most effective for long-term tumor control.

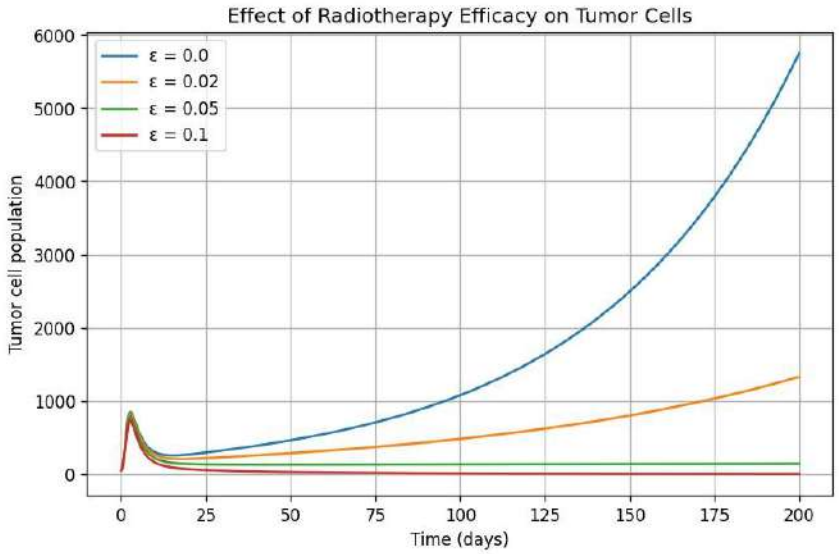

Figure 4. Effect of radiotherapy efficacy ε on tumor cells T(t). Curves correspond to ε = 0.0,0.02,0.05,0.1.

Figure 4 illustrates the threshold role of ε. Without treatment ($\varepsilon = 0.0$), tumor growth is unchecked. At $\varepsilon = 0.02$, growth slows but persists. At $\varepsilon = 0.05$, partial suppression occurs, while $\varepsilon = 0.1$ nearly eradicates the tumor. This confirms the analytical condition that tumor eradication requires reducing R_0 below one.

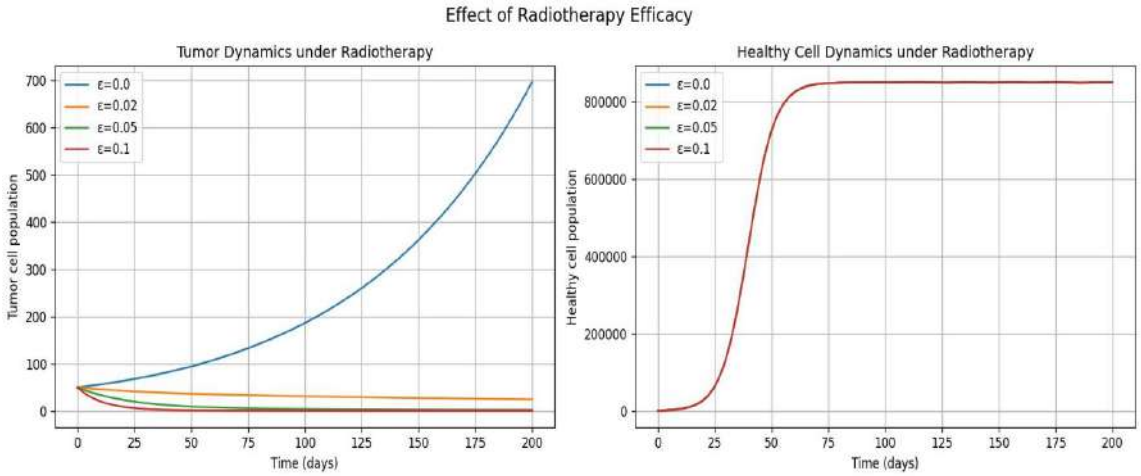

Figure 5. Radiotherapy efficacy ε and its effect on T(t) (left) and H(t) (right).

Figure 5 shows that radiotherapy efficacy alters tumor dynamics while leaving healthy cell recovery largely unchanged. For all values of ε, $H(t)$ returns to its carrying capacity, demonstrating selective tumor suppression.

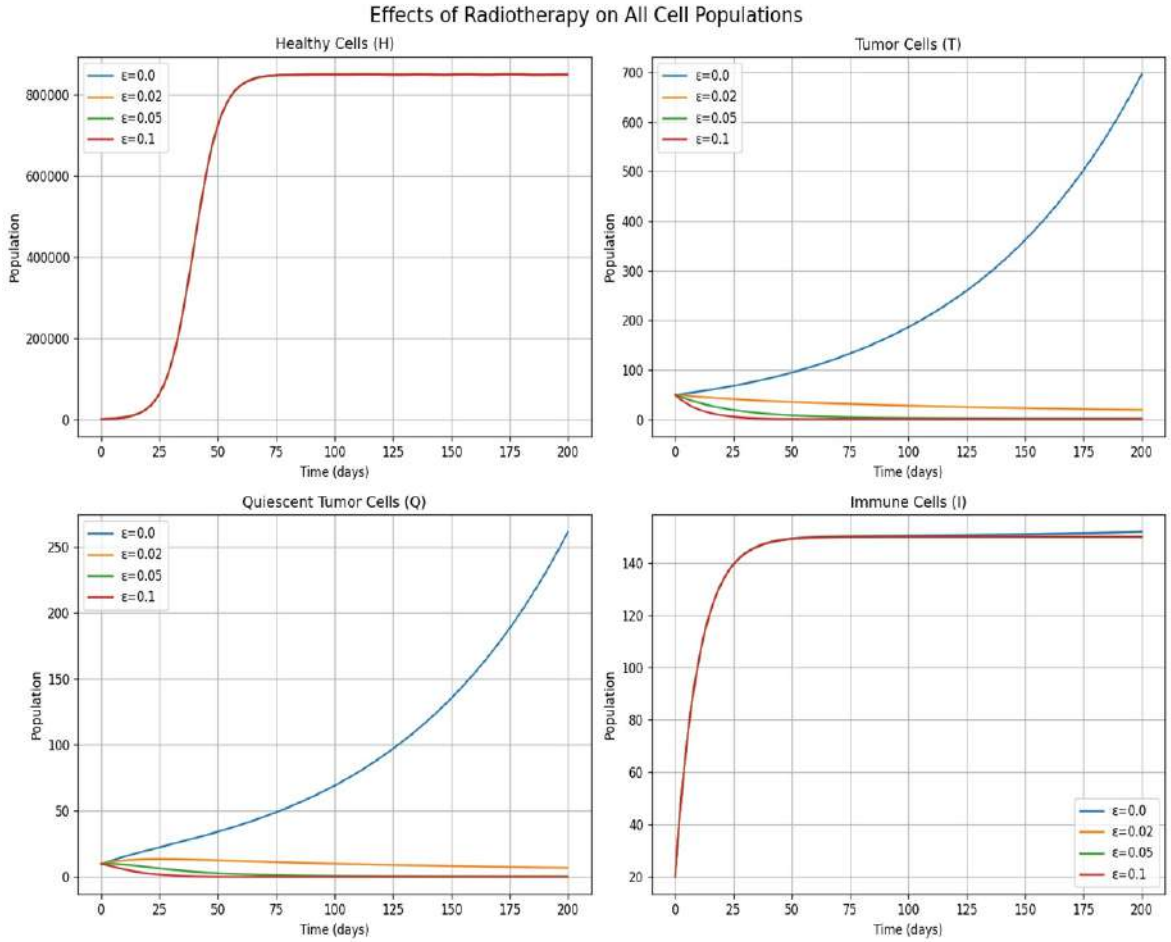

Figure 6. Effect of radiotherapy efficacy ε on all compartments: H(t), T(t), Q(t), I(t).

Figure 6 confirms that radiotherapy strongly reduces $T(t)$ and $Q(t)$, while $H(t)$ and $I(t)$ remain stable. Thus, the treatment primarily targets malignant cells in this model.

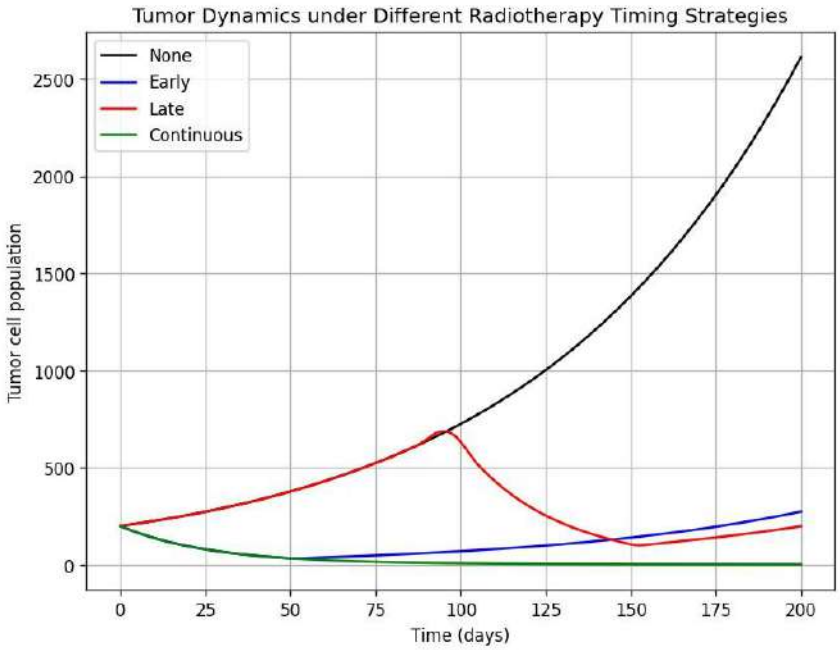

Figure 7. Tumor trajectories under no treatment, early therapy, late therapy, and continuous therapy.

4.3. Treatment Timing

Figure 7 demonstrates the influence of timing. Early therapy suppresses tumors before they expand, while late therapy reduces tumor size but leaves residual populations. Continuous therapy maintains near-zero tumor levels throughout.

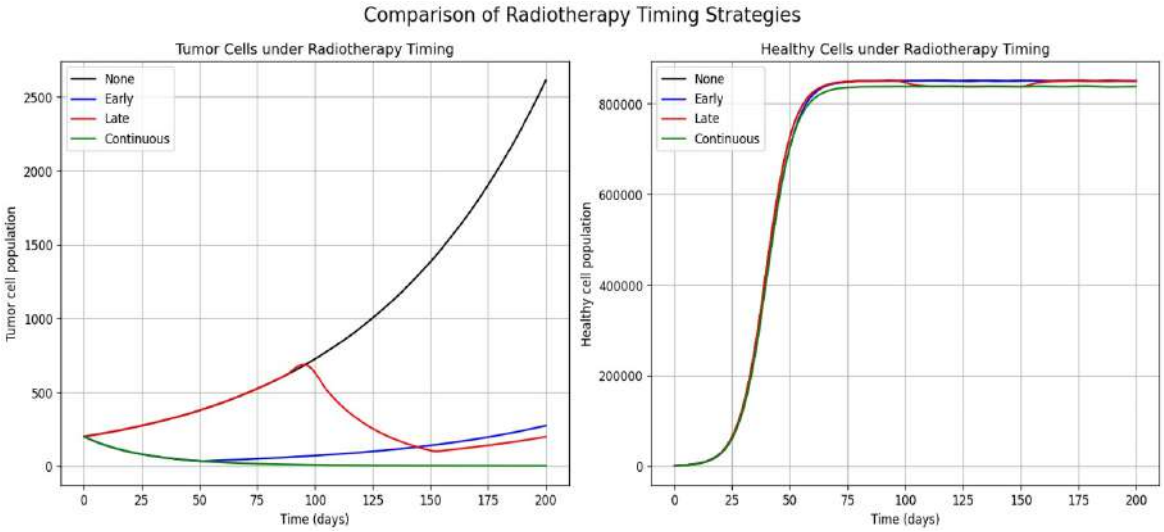

Figure 8. Comparison of radiotherapy timing: tumor dynamics (left) and healthy cells (right).

Figure 8 highlights that tumor suppression depends strongly on timing, while healthy cells $H(t)$ are robust and recover regardless of schedule.

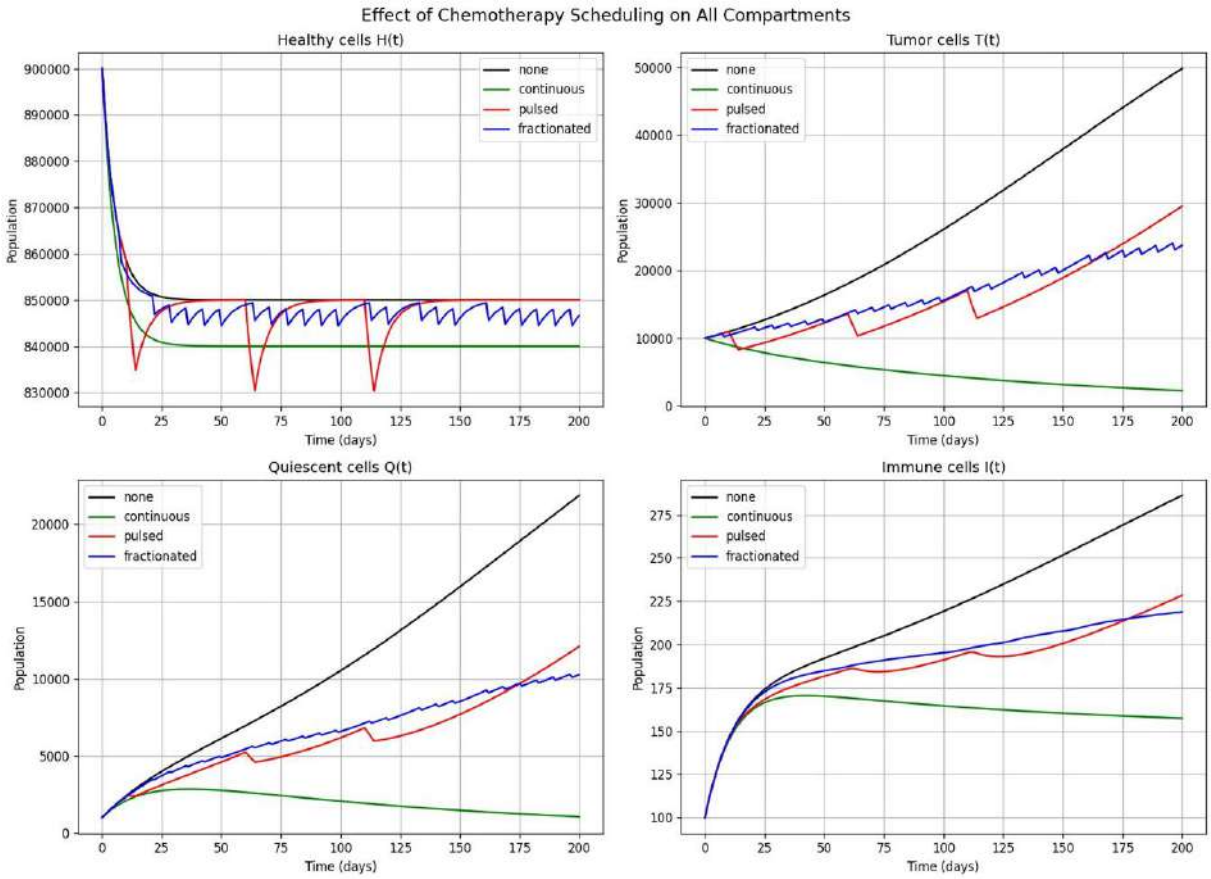

Figure 9. Chemotherapy schedules: no therapy, continuous, pulsed, and fractionated. Effects shown for all cell populations.

4.4. Chemotherapy Effects

Figure 9 shows that continuous chemotherapy best suppresses $T(t)$ and $Q(t)$. Pulsed chemotherapy produces oscillations, while fractionated therapy only partially controls growth. Healthy and immune cells remain relatively stable, though continuous therapy slightly reduces $H(t)$ compared to no therapy.

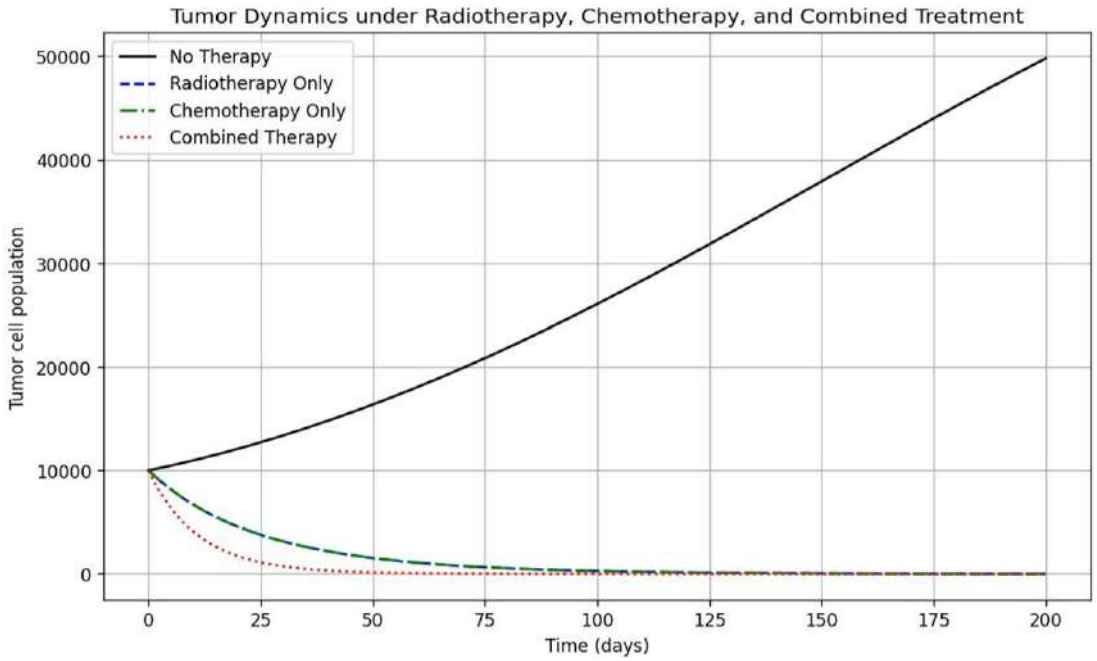

Figure 10. Comparison of tumor trajectories under no therapy, radiotherapy alone, chemotherapy alone, and combined therapy.

4.5. Combined Therapies

Figure 10 shows that radiotherapy and chemotherapy alone reduce tumor burden, but their combination achieves the most rapid and complete suppression.

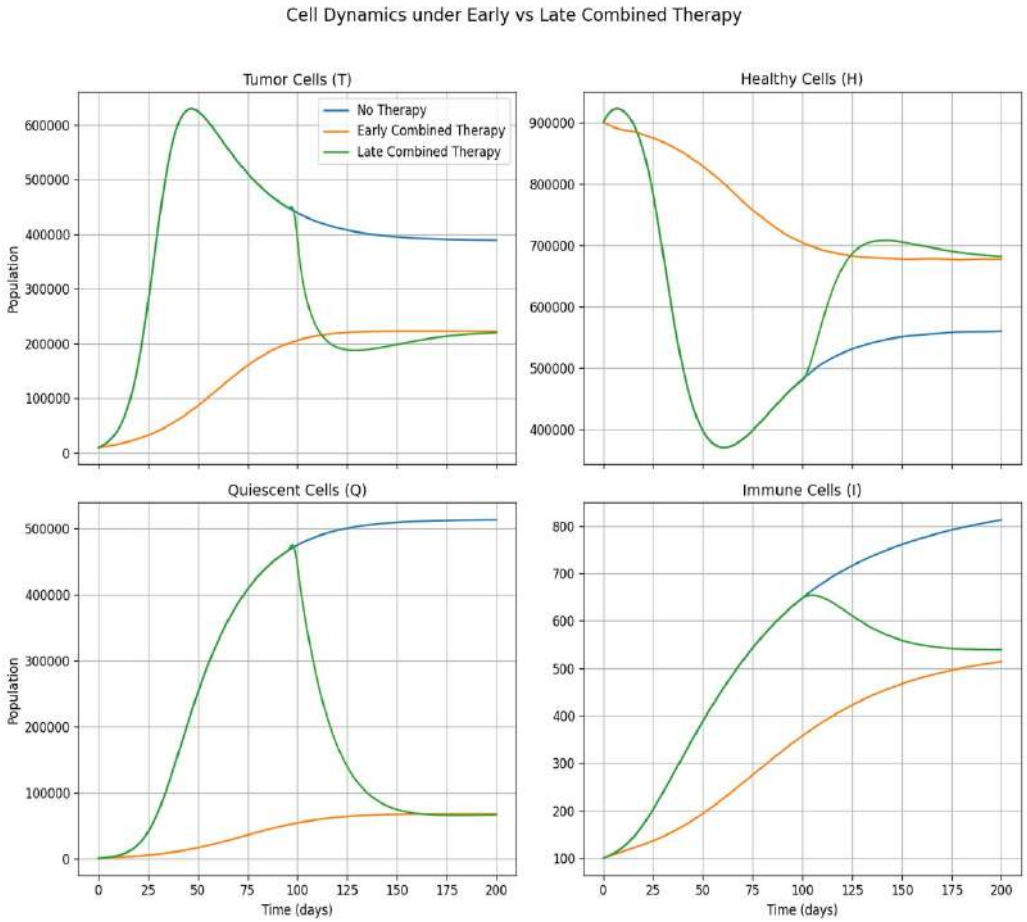

Figure 11. Cell dynamics under early versus late combined therapy compared with no therapy.

Figure 11 illustrates that early combined therapy is more effective, maintaining low tumor and quiescent populations with fewer oscillations, whereas late combined therapy results in higher peaks and larger fluctuations across compartments.

5. DISCUSSION

This study examined a nonlinear model describing interactions among healthy cells, tumor cells, quiescent cells, and immune cells under radiotherapy and chemotherapy. The analytical results show that the system remains positive and bounded for all biologically meaningful initial conditions. This confirms that the model structure reflects realistic cell population dynamics and avoids unphysical behaviors such as negative or unbounded growth.

The stability analysis established that the tumor-free equilibrium becomes globally asymptotically stable when the basic reproduction number is less than one. In this regime, treatment and immune activity are strong enough to suppress tumor growth and drive the system toward a healthy steady state. The result aligns with earlier work showing that tumor–immune systems can switch between persistence and elimination depending on a threshold balance between proliferation and immune-mediated killing [3, 4]. The presence of quiescent cancer cells does not change the core threshold structure but can delay convergence to the tumor-free state, reinforcing the clinical observation that dormant cells contribute to long-term relapse.

When $(R_0 > 1)$, the model predicts sustained tumor presence despite immune activation and treatment exposure. This outcome is consistent with studies showing that insufficient immune pressure or suboptimal therapy allows tumors to persist or rebound [5, 6]. The inclusion of quiescent cells captures the reduced sensitivity of non-proliferating cells to therapy, a feature widely noted in radiotherapy and chemotherapy modeling [7, 26]. These cells form a reservoir that can repopulate the tumor, highlighting the need for treatment strategies that effectively target both active and dormant populations.

Sensitivity analysis identified the parameters that most strongly influence tumor persistence. Higher radiotherapy efficacy, stronger immune killing, and increased activation of immune cells reduce tumor survival. In contrast, higher tumor proliferation and faster transition to quiescence increase tumor resilience. These findings support observations from radiotherapy and immunotherapy studies, where enhanced cytotoxicity and improved immune activation correlate with better outcomes [27, 28]. The results also suggest that optimizing therapy schedules may shift system dynamics across the $(R_0 = 1)$ threshold, improving treatment success.

The model provides a useful framework for understanding how treatment and immune activity interact, but several limitations remain. The system does not include spatial effects, angiogenesis, or detailed pharmacokinetics, all of which can influence treatment outcomes. Radiotherapy and chemotherapy are modeled as time-dependent killing functions rather than through dose distribution or repair mechanisms. The immune response is simplified and does not incorporate regulatory cells or cytokine signaling. These omissions keep the model tractable but limit its ability to reproduce complex biological responses.

Future work may extend the model by incorporating adaptive therapy strategies, dose-fractionation schemes, or more detailed immune mechanisms. Parameter calibration using patient-specific data would allow exploration of personalized treatment planning. Spatial extensions using partial differential equations or agent-based models can capture heterogeneity in tumor structure and microenvironmental effects.

Overall, the results demonstrate how mathematical models can clarify the balance between tumor proliferation, immune regulation, and treatment strength. The stability threshold and sensitivity findings provide a foundation for designing optimized treatment strategies and highlight the potential for using mathematical models to guide personalized cancer therapy.

6. CONCLUSION

This study developed and analyzed a nonlinear model describing interactions among healthy cells, tumor cells, quiescent cells, and immune cells under radiotherapy and chemotherapy. The analysis showed that the system remains positive and bounded for all biologically meaningful initial conditions. The tumor-free equilibrium is globally asymptotically stable when the basic reproduction number $(R_0 < 1)$, indicating conditions under which treatment and immune response are sufficient to eliminate the tumor. Sensitivity analysis identified key parameters governing tumor persistence, including radiotherapy efficacy, chemotherapy strength, immune-killing capacity, and tumor proliferation rates. The results showed that increasing radiotherapy effectiveness and strengthening immune-mediated killing reduce tumor survival, while high tumor proliferation and quiescence transition rates promote persistence. The findings highlight how mathematical models can clarify the interplay between tumor growth, immune regulation, and therapeutic interventions. The model provides a useful framework for evaluating treatment strategies and supports the design of personalized and optimized therapeutic regimens.

Funding: This study received no specific financial support.
Institutional Review Board Statement: Not applicable.
Transparency: The authors state that the manuscript is honest, truthful, and transparent, that no key aspects of the investigation have been omitted, and that any differences from the study as planned have been clarified. This study followed all writing ethics.
Competing Interests: The authors declare that they have no competing interests.
Authors' Contributions: All authors contributed equally to the conception and design of the study. All authors have read and agreed to the published version of the manuscript.

REFERENCES

[1] A. K. Laird, S. A. Tyler, and A. D. Barton, "Dynamics of tumor growth: A mathematical analysis," *British Journal of Cancer*, vol. 19, no. 2, pp. 278–291, 1965.

[2] L. Norton, "A Gompertzian model of human breast cancer growth," *Cancer Research*, vol. 48, no. 24, pp. 7067-7071, 1988.

[3] V. A. Kuznetsov, I. A. Makalkin, M. A. Taylor, and A. S. Perelson, "Nonlinear dynamics of immunogenic tumors: Parameter estimation and global bifurcation analysis," *Bulletin of Mathematical Biology*, vol. 56, no. 2, pp. 295-321, 1994. https://doi.org/10.1007/BF02460644

[4] D. Kirschner and J. C. Panetta, "Modeling immunotherapy of the tumor–immune interaction," *Journal of Mathematical Biology*, vol. 37, no. 3, pp. 235-252, 1998. https://doi.org/10.1007/s002850050127

[5] L. G. De Pillis, A. E. Radunskaya, and C. L. Wiseman, "A validated mathematical model of cell-mediated immune response to tumor growth," *Cancer Research*, vol. 65, no. 17, pp. 7950–7958, 2005. https://doi.org/10.1158/0008-5472.CAN-05-0564

[6] J. Arciero, T. Jackson, and D. Kirschner, "A mathematical model of tumor-immune evasion and siRNA treatment," *Discrete and Continuous Dynamical Systems Series B*, vol. 4, no. 1, pp. 39-58, 2004.

[7] T. Garner, D. S. Salazar, and J. Whitman, "Mathematical analysis of quiescent and proliferating cell interactions," *Mathematical Biosciences*, vol. 201, no. 1–2, pp. 110–126, 2006.

[8] S. Baykara and M. A. Onur, "Cancer as a condition of uncontrolled cellular proliferation: A mathematical perspective," *Journal of Cancer Research Updates*, vol. 4, no. 2, pp. 45–52, 2015.

[9] R. M. Anderson and R. M. May, *Infectious diseases of humans: Dynamics and control*. United Kingdom: Oxford University Press, 1991.

[10] Y. Liu and C. Yang, "Lotka–Volterra modeling of tumor–host cell competition," *Applied Mathematical Modelling*, vol. 39, no. 15, pp. 4518–4532, 2015.

[11] Y. Wang, H. Liu, and Z. Zhao, "Mathematical modeling of radiotherapeutic tumor control incorporating immune response," *Computational and Mathematical Methods in Medicine*, 2020.

[12] R. Baskar, K. A. Lee, R. Yeo, and K.-W. Yeoh, "Cancer and radiation therapy: Current advances and future directions," *International Journal of Medical Sciences*, vol. 9, no. 3, pp. 193-199, 2012. https://doi.org/10.7150/ijms.3635

[13] V. T. DeVita, T. S. Lawrence, and S. A. Rosenberg, *DeVita, Hellman, and Rosenberg's cancer: Principles and practice of oncology*, 8th ed. United States: Lippincott Williams & Wilkins, 2008.

[14] P. Van den Driessche and J. Watmough, "Reproduction numbers and sub-threshold endemic equilibria for compartmental models of disease transmission," *Mathematical Biosciences*, vol. 180, no. 1-2, pp. 29-48, 2002. https://doi.org/10.1016/S0025-5564(02)00108-6

[15] J. O. Ochwach, M. O. Okongo, and M. M. Muraya, "Mathematical modeling of host-pest interac-tions in stage structured populations: A case of false codling moth [Thaumatotibia leucotreta]," *Journal of Progressive Research in Mathematics*, vol. 18, no. 4, pp. 1-21, 2021.

[16] O. Jimrise, M. Okongo, and M. Muraya, "Stability analysis of a sterile insect technique model for controlling false codling moth," *Journal of Mathematical Analysis and Modeling*, vol. 4, no. 1, pp. 78-105, 2023.

[17] M. Robertson-Tessi, A. El-Kareh, and A. Goriely, "A mathematical model of tumor–immune interactions," *Journal of Theoretical Biology*, vol. 294, pp. 56-73, 2012. https://doi.org/10.1016/j.jtbi.2011.10.027

[18] D. Wodarz and N. L. Komarova, *Dynamics of cancer: Mathematical foundations of oncology*. Singapore: World Scientific, 2014.

[19] R. A. Gatenby and P. K. Maini, "Cancer modelling: Integrating biology and mathematics," *Nature Reviews Cancer*, vol. 3, pp. 828–838, 2003.

[20] R. Eftimie, J. L. Bramson, and D. J. D. Earn, "Interactions between the immune system and cancer: A brief review of non-spatial mathematical models," *Bulletin of Mathematical Biology*, vol. 73, no. 1, pp. 2-32, 2011. https://doi.org/10.1007/s11538-010-9526-3

[21] P. Sharma and J. P. Allison, "The future of immune checkpoint therapy," *Science*, vol. 348, no. 6230, pp. 56–61, 2015. https://doi.org/10.1126/science.aaa8172

[22] K. P. Wilkie and P. Hahnfeldt, "Mathematical models of immune-induced cancer dormancy and the emergence of immune evasion," *Interface Focus*, vol. 3, no. 4, p. 20130010, 2013. https://doi.org/10.1098/rsfs.2013.0010

[23] P. S. Kim, P. P. Lee, and D. Levy, "Mathematical modeling of tumor–immune interactions: A survey of models, analysis, and applications," *Bulletin of Mathematical Biology*, vol. 76, no. 4, pp. 865–911, 2014a.

[24] K. S. Kim, G. Cho, and I. H. Jung, "Optimal treatment strategy for a tumor model under immune suppression," *Computational and Mathematical Methods in Medicine*, vol. 2014, no. 1, p. 206287, 2014. https://doi.org/10.1155/2014/206287

[25] J. O. Ochwach, O. O. Mark, and A. L. M. Murwayi, "On basic reproduction number r0: Derivation and application," *Journal of Engineering and Applied Sciences Technology*, vol. 173, pp. 2-14, 2023.

[26] P. Hahnfeldt, D. Panigrahy, J. Folkman, and L. Hlatky, "Tumor development under angiogenic signaling: A dynamical theory of tumor growth, treatment response, and postvascular dormancy," *Cancer Research*, vol. 59, no. 19, pp. 4770-4775, 1999.

[27] H. Enderling, A. R. A. Anderson, M. A. J. Chaplain, A. J. Munro, and J. S. Vaidya, "Mathematical modelling of radiotherapy strategies for early breast cancer," *Journal of Theoretical Biology*, vol. 241, no. 1, pp. 158-171, 2006. https://doi.org/10.1016/j.jtbi.2005.11.015

[28] R. Serre, S. Benzekry, and L. Padovani, "Mathematical modeling of immunotherapy combined with radiotherapy," *Cancer Research*, vol. 76, no. 15, pp. 4483–4493, 2016.